

A meso-scaled simulation on the thickness effect of two-dimensional triaxially braided composites under tensile loads

Yang Bai^{a,c}, Liu Peng^{a,c}, Zhao Zhenqiang^{a,c*}, Zhang Chao^{a,b,c*}

^aSchool of Aeronautics, Northwestern Polytechnical University, Xi'an, 710072, China

^bSchool of Civil Aviation, Northwestern Polytechnical University, Xi'an, 710072, China

^cKey Laboratory of Civil Aviation in Aircraft Impact Protection and Safety Assessment, Northwestern Polytechnical University, Xi'an, 710072, China

Abstract

Two-dimensional traxially braided composite (2DTBC) has been proved to own better integration and impact resistance than traditional laminate. This study investigates the mechanical behavior of 2DTBC, focusing on the effects of specimen thickness through experimental and simulation methods. Tension tests were conducted on specimens of varying thicknesses using a universal test machine, revealing significant differences in mechanical response between axial and transverse orientations. Simulation based on a previously proposed elastoplastic constitutive provided insights into failure mechanisms and damage characteristics, elucidating the impact of thickness on load-bearing capacity and strength. Results indicate that axial specimens exhibit more uniform strain distribution across thicknesses, whereas transverse specimens show localized damage and strain concentration at bias fiber boundaries. The study underscores the critical role of thickness in determining the mechanical properties and failure modes of 2DTBC, offering valuable insights for optimizing structural design and performance in composite materials.

Keywords: 2DTBC, Tensile, Thickness, Elastoplastic, Simulation

1. Introduction

Under the demand for high performance and lightweight design for materials utilized in the aerospace field, braided composites have become widely applied on account of their structural stability and distinguished impact damage resistance compared to traditional unidirectional laminated composites. The two-dimensional triaxial braided composites (2DTBC) also demonstrate better in-plane quasi-isotropic properties compared to 2D woven composites [1]. Typical applications, such as in engine casings, fan blades, and other structures on aircraft, pose impact safety challenges for braided composites.

Researches have shown that the strength of a composite material is sensitive to the size of the coupon specimen. For traditional unidirectional composites, Wisnom[2] and other researches[3] have conducted tension, compression and flexure tests and reported a weakened mechanical response with larger specimen sizes. Braided composites, however, exhibited different conclusions, Zhang[4] et al. and Zhao[5] et al. investigated the behavior of 2DTBC with different specimen widths and found an increasing strength in wider specimens, which is distinct from laminated composites. Cai[6] et al.

used simulation methods and attributed the size effect to free-edge effect and transformed failure mode. Few studies pay attention to discrepancy introduced by different thickness on the performance of 2DTBC. It is inevitable to involve the structure design with different thickness, so the determination of realistic effective mechanical is crucial for engineer application.

A combination of experimental and simulation methods was applied to acquire the mechanical behavior of 2DTBC. In this study, tension specimens of 2DTBC along axial and transverse directions were designed and experimentally investigated under quasi-static condition using universal testing machine. After validation of the finite element methods (FEM), the failure behavior was compared and analyzed based on numerical results, which expand the understanding of thickness effect on the 2DTBC.

2. Specimen description and experiment methods

The composite material investigated in this paper is composed of 3266 epoxy resin and T700 carbon fiber, originating from the same manufacturer as referenced in previous literature. The geometry and braided structure of this 2DTBC are illustrated in Figure 1(a), consisting of axial fiber tows along the 0° direction and bias fiber tows at a 60° angle relative to the axial fiber tows. The axial fiber tows and bias fiber tows have filament counts of 24K and 12K, respectively. The parameters of each component are obtained from the literature [7] and summarized in Table 1. Panels with an overall fiber volume ratio of approximately 56% were formed into different thicknesses, consisting of 1 layer, 2 layers, and 3 layers, respectively, for the tension experiment. The thickness of a single layer is about 0.57 mm. The axial and transverse specimens were cut into "dog bone" shapes from the preformed panel. In the subsequent sections, a specimen with 1 layer along the axial direction is referred to as "1L-A". Other specimen conditions are named as 1L-T, 2L-A/T, and 3L-A/T, respectively.

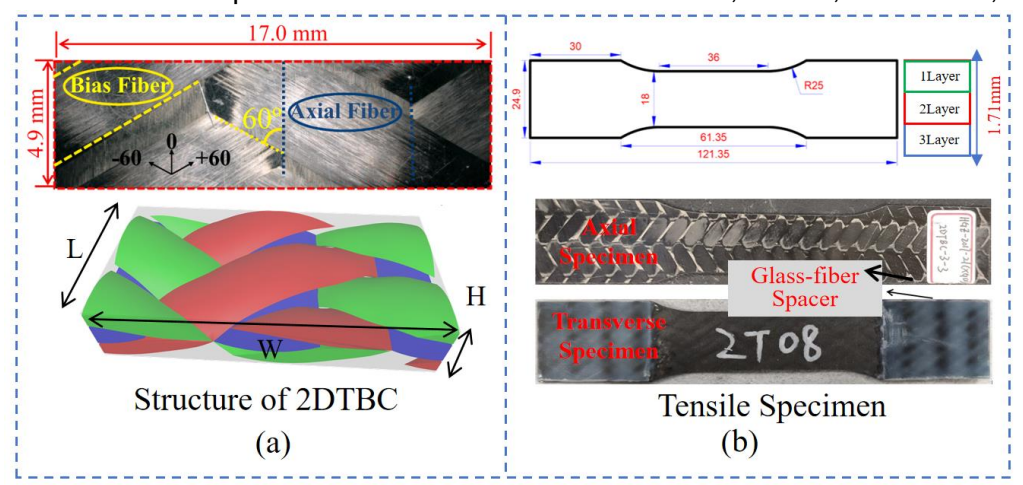


Figure 1-(a) Braided structure and unit cell of 2DTBC (b) Dimension of axial and transverse tensile specimen of 2DTBC

Table 1 Properties of epoxy resin and fibers of 2DTBC

Property	Carbon fiber/T700	Epoxy resin/3266
Density, g/cm3	1.8	1.2
Axial modulus, GPa	230	2.5
Transverse modulus, GPa	15	2.5

Shear modulus, GPa	27	0.96
Poisson ratio	0.2	0.3

A hydraulic servo universal machine with a loading capacity of 200KN is used to apply tension loads to the specimen for quasi-static test, as shown in Figure 2. The loading speeds are held at 1.68 mm/min for "dog bone" sized specimen to reach a strain rate of 10-3/s. The deformation field of the specimen during the test is measured by an optical camera. Two methods are used to acquire the strain value of the specimen which are Digital image correlation and strain gauge separately. One side of the specimen is sprayed with speckle and the strain gauge is attached to the other side. The effectiveness of the DIC results can be verified by comparing with strain gauge values. Additionally, two infrared cameras are employed to monitor the variation in the temperature field of the specimen and for mutual verification. One is FLIR X6520sc infrared camera (Temperature range – 40 to 650 °C, error of ±2 °C) with a resolution of 640 × 480 pixels and a frame rate of 500Hz, the other is FLIR-A655SC with a resolution of 480× 148 pixels and a frame rate of 50Hz.

3. Implementation of numerical methods of 2DTBC

3.1 Elastoplastic progressive damage constitutive model

Firstly, as presented in Figure 3(a), the two components, epoxy resin and the fiber tow, are determined to be isotropic and transversely isotropic materials, respectively. The mechanical behaviors of the pure matrix and fiber tows both are considered to be elastoplastic response and progressive damage characterization. The Hill yield criterion [8] fits to describe the fiber tow performance and pure matrix is expressed using J2 flow theory [9]. The concrete damage initiation and evolution criterion of fiber tow and pure matrix could refer to previous study [7]. Cohesive elements are also introduced to simulate delamination phenomenon of interface, and the quadratic nominal stress criterion [10] and Benzeggagh–Kenane fracture criterion is recommended [11,12] and utilized to characterize element response.

3.2 Modeling the tensile finite element model of 2DTBC

The elastoplastic progressive damage model of fiber yarns and matrix is numerically implemented in the commercial FE software ABAQUS/ Standard through an integrated user-defined subroutine VUMAT. The geometry model is established using TEXGEN software, as depicted in Figure 1 (b). The "dog bone" sized specimen was created and modified using Hypermesh software, with each component presented in Figure 3(b). Similar the quasi-static specimen in experiment, the degrees of freedom of the left side in x, y and z directions and right side in y and z directions are totally fixed constraints. A displacement of 2mm is applied to the right set in the x direction to simulate the quasi-static experimental load.

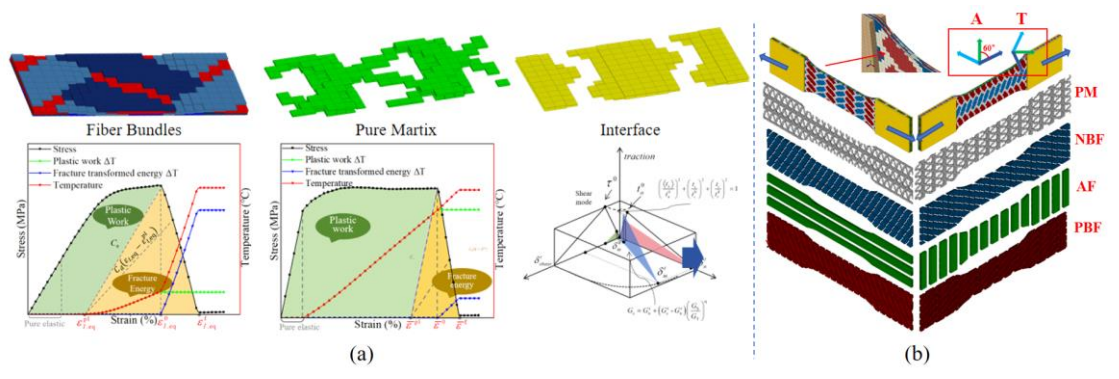


Figure 3-(a) Elastoplastic constitutive model of 2DTBC component (b) "Dog bone" sized tensile specimen simulated model

4. Result and discussion

4.1 Experiment result of 2DTBC

4.1.1 Mechanical response of tension tests

Figure 4 presents typical stress-strain curves axial and transverse specimen of 2DTBC with different thickness under quasi-static loads. The axial specimen exhibits a linear response, consistent with findings reported by Cai[6]. This behavior is attributed to the totally straight axial fiber along loading direction, known for their inherently brittle performance. Conversely, an obvious stiffness reduction is observed in transverse specimen in the early strain stage. This non-linear response is contributed to the inelastic behavior of pure matrix and transverse damage of fiber tows[13]. Eventually, damage accumulation induced the breakage of fiber tow and the specimen suddenly unloads, with the peak stress representing its ultimate strength. Subsequently, the specimen loses the carrying capacity and completely failed. For comprehensive understanding, the mechanical response of 8 layers' specimen from our previous study was also concluded for comparison.

The averaged strength and failure strain are summarized in Table 2. An obvious increase is observed in the strength in both axial specimen and transverse specimen. The strength increases by approximately 20.7%, 28.5% and 35.1% as the number of layers contained change from 1 layer to 2 layers, 3layers and 8layers, respectively. As for the transverse specimen, the strength increases about 38.5%, 51.1% and 143.4% for 2T, 3T and 8T specimens. The failure strain of 2DTBC with different thickness shows little variation under axial direction loads, while a slight increase is observed in transverse specimen. Similar trends have been reported in other studies on 2DTBC[13] when the number of unit-cells increased from 2 to 8. It is concluded that the axial specimen is less sensitive to the thickness of specimen compared to transverse specimen, although the strength of both two kinds of specimen exhibits a weakening increase tendency.

It is noticed that the stiffness of 2DTBC is not sensitive to the thickness of the specimen. Additionally, the properties of axial specimen are much greater than that of the transverse specimen. This phenomenon is determined by the braided structure, bias fiber in transverse specimen is fluctuant and deflecting from the loading direction, which lead to a loss in mechanical performance.

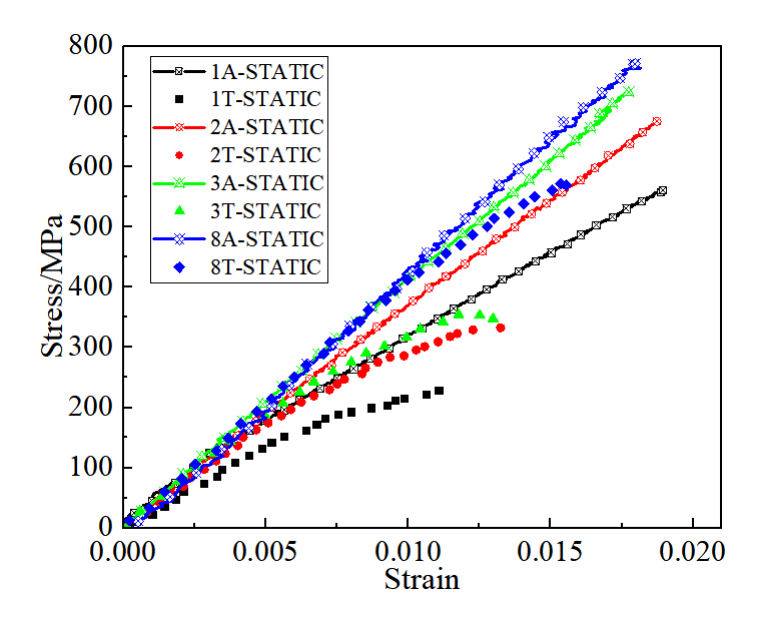


Figure 4-Stress-strain curve of 1L, 2L, 3L and 8L specimen under quasi-static loads

Table 2 Summary of the averaged strength and failure strain of 2DTBC under different loads

Specimen number	Ехр-/МРа	Sim-/MPa	Error/%	Failure strain
1A-10-3/s	564±0.2	572±0.8	1.4	0.0190
1T-10-3/s	231±0.1	254 ± 0.3	9.0	0.0114
2A-10-3/s	681±0.8	725±0.9	6.1	0.0187
2T-10-3/s	320 ± 0.9	350 ± 0.5	8.6	0.0130
3A-10-3/s	725±0.5	716±0.7	1.2	0.0181
3T-10-3/s	349 ± 0.4	355±0.3	1.7	0.0135
8A-10-3/s	762 ± 0.8			0.0179
8T-10-3/s	563±0.8			0.0156

4.1.2 Failure behavior of 2DTBC

During the quasi-static experiment, the specimen generally fails in an instant collection point, and then unload immediately. The final failure characterization of 1A, 1T, 2A, 2T 3A and 3T specimen is compared in Figure 5 to examine the difference brought by thickness.

For axial specimen, the damage is concentrated at the boundary between gauge section and arc segment, appearing in a form of V-shaped. And the location of failure includes primary part and subordinate parts, distributed along the braided structure. In the primary part, the matrix between fibers destroyed and the bias fiber are separated by tensile stress perpendicular to the fiber direction. From the aspect of thickness direction, obvious delamination of interface exists between yarns and matrix, along with axial fiber breakage. With the increase of thickness, the overall degree of damage becomes more severe, as shown in 3 layers' specimen, where the expanded range of damage is longer. A large amount of matrix crack and fiber breakage absorbs more fracture energy and finally, ultimately resulting in higher strength. The dominant failure mode is not affected by changes in specimen thickness.

In Figure 5(b), the failure morphology of transverse specimens with different thickness are compared. The damage location disperses along the gauge section and concentrate at the intersection of negative bias fiber and positive bias fiber. Similar to the axial tension condition, matrix crack, interface delamination and fiber breakage still occurred. As thickness increase, the disseminated damage become more centralized and locally aggravated, which can be determined in photos along thickness direction. It is noted that the failure of transverse specimen firstly experienced matrix crack located at free-edge, followed by final fiber breakage leading to unloading.

The amplification of damage is presented in Figure 5(c) providing a profound understanding of failure

mechanism of 2DTBC. In the axial specimen, the axial fiber is directly cut off by tension load accompanied by little transvers splitting. The bias fiber basically exhibits transverse separation because of the load transmitting from adjacent axial fiber. Significant difference in bias fiber damage are captured in transverse specimen. The bias fiber, oriented at 30 degrees to the loading direction, experiences both fiber breakage and transverse splitting. Meanwhile, the axial fiber, being perpendicular to the loading direction, is destroyed only in the form of transverse fracture. These distinct phenomena collectively lead to variations in mechanical response.



Fig. 5 (a) Damage characterization comparison of axial specimen (b) Damage characterization comparison of transverse specimen (c) Clarification of damage mode under different loading condition

4.2 Validation of the FE model

Figure 6 compares the experimental and simulated response, specifically highlighting the damage of fiber tension and strain field distribution for verification. And the predicted strength as well as errors are summarized in Table.2. The averaged error in strength prediction is below 5% and the stiffness matches well with the test results in the early strain stage (before the strain reaches 0.3%). The fiber tension damage at the failure stage in the simulation is presented in the middle of Figure 7, the damage of simulating result similarly includes a primary part and secondary part in axial specimen and the position concentrate at the transition section. The strain field of distribute along the braided structure and correlated well with the DIC result. With regard to the transverse specimen, the failure mode is constant with test result which occurred at the intersection edge of two bias fiber. Strain of and DIC result when the global strain reached 0.5% both indicated the phenomenon of free-edge effect. Strain concentration is located at the end of bias fiber near the free boundary and warping behavior initiated from the edge is also captured.

The comparison of the above results validates that the proposed elastoplastic constitutive model can precisely predict the tensile response of 2DTBC specimen. Based on the simulating method, the underlying failure mechanism and damage characteristic could be revealed in the section of 4.3.

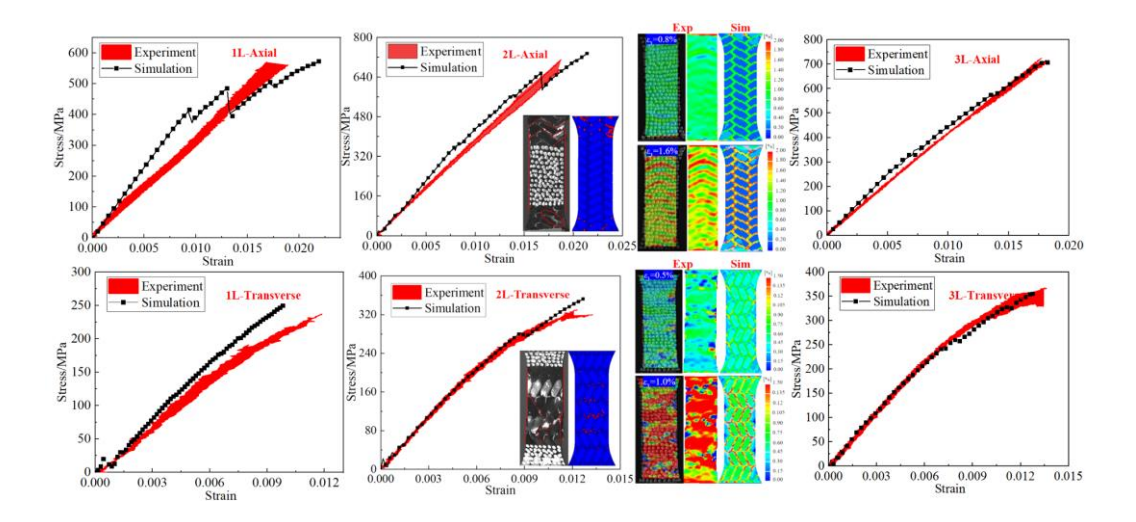


Figure 6-Validation of the FE model for 2DTBC with different thickness

4.3 Numerical simulation characterization on the failure behavior of 2DTBC

After verification, the simulated damage result of the 3 layers' specimen at unloading point is presented as example in Figure 7. Different kinds of failure mode are named in the top frame. Primarily, the corresponding fiber tensile damage dominates the failure and correlated well with the specimen. The damage accumulating process is investigated, and the occurrence sequence is numbered in figures.

For the axial specimen, severe transverse matrix tension damage in fiber tows first occurs in the bias fiber and less MT damage is subsequently found in axial fibers. Then, the delamination damage initiates at both intra-layer and inter-layer interfaces. Matrix compression damage is minimal and can be ignored, while the ductile damage in pure matrix is recorded to concentrate at arc segment of the specimen. Almost simultaneously, axial fiber tension damage also occurred without the support of surrounding matrix accompanied by few BFT damage. It is noted that the location of interface damage still located at the arc segment which can be speculated that the accumulation of matrix cracking, interface failure contributed most to the fiber breakage.

The same failure regularity is also captured for transverse specimen. The difference is that axial matrix tension(AMT) initiates first and almost completely destroyed at peak strength. Additionally, matrix compression damage in fibers is obviously much more than axial specimen. The negative and positive bias fiber tension damage is separately displayed, occurring mostly at the fluctuating positions of the yarn, where shear stress easily concentrates.

In general, the final fiber breakage determines the ultimate difference of axial and transverse specimen. Several types of failure such as matrix crack, interface failure and pure matrix ductile damage, occur and aggravate the damage. The specimen can absorb more energy through crack and fracture thus exhibits higher strength.

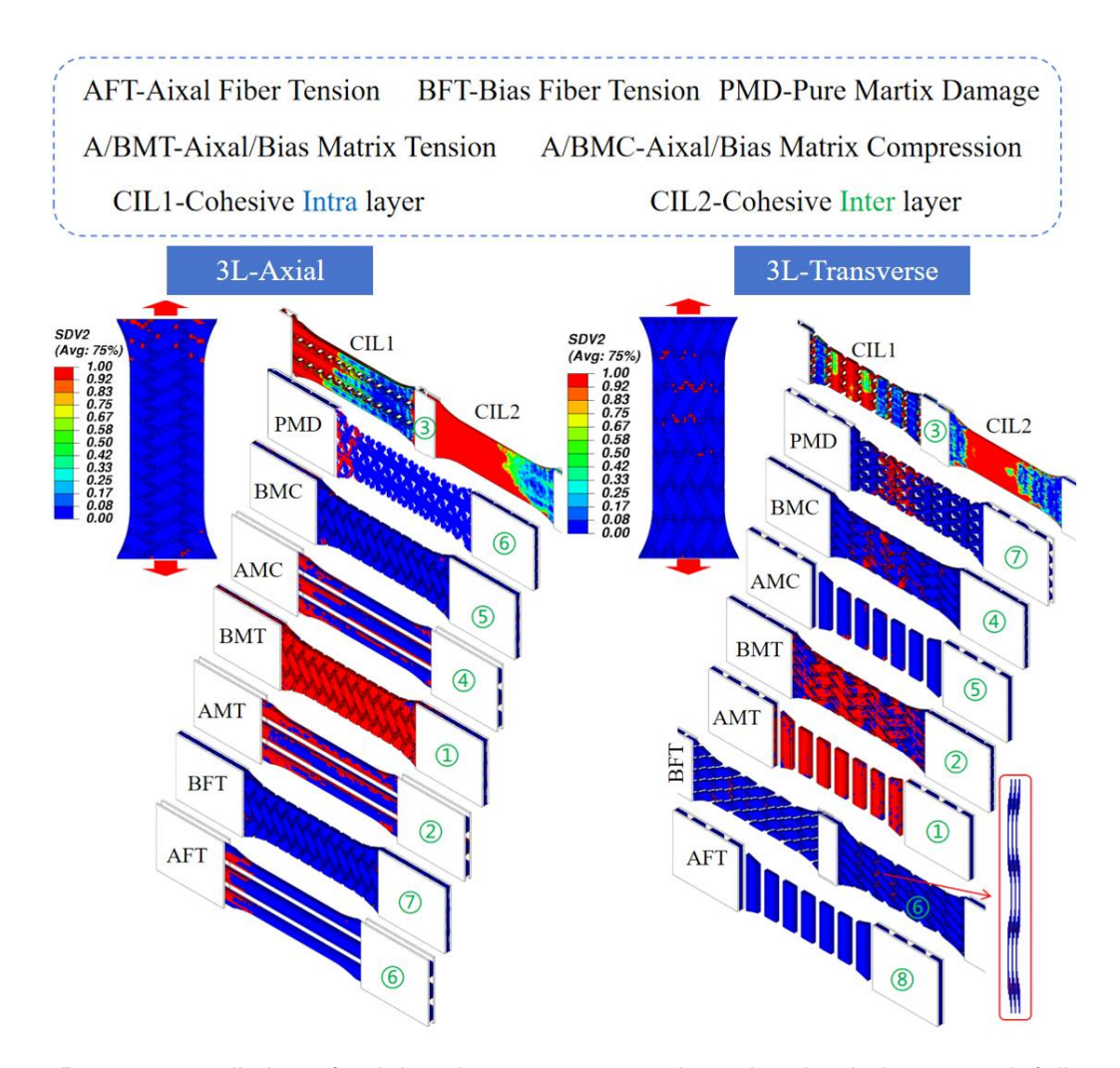


Figure 7-Damage prediction of axial and transverse specimen by simulation at peak failure point 4.4 Thickness effect discussion

The macro response differences of 2DTBC with different thickness stem from the micro- and mesoscale damage discrepancies. Through the simulation method, the inner mechanism of thickness effect is revealed, as shown in Figure 8.

Strain \mathcal{E}_{yy} of axial specimen and transverse specimen with different thickness is compared in Figure 8(a). For axial specimen, the strain distribution along thickness direction is uniform, resembling a stacking mode. Different layers exhibit similar structure-based strain field, indicating that the axial specimen is less sensitive to the thickness change of specimen. As for the damage in Figure 8(b), there are more axial fiber tension damage in 3 layers' specimen. The larger content of fiber breakage damage enhances the resistance under tensile loads. Same conclusion is also reported by Bai et al[14]. Load transmission and bearing through layers is also the consequence of better performance.

The transverse specimen is relatively susceptible to thickness effect. As shown on the right of Figure 8(a), the strain pattern is irregular and not simply repetitive stacking. The deformation of the component is asymmetrical, and the surface strain concentration is more severe at the boundary of bias fiber. 3 layers' specimen is more easily damaged in local position compared to 1LT specimen. Localized and abundant fiber breakage along 3 layers promotes the response than that of 1LT specimen.

It is noted that the simulation represents an ideal loading condition, the strain is periodic along loading direction which hardly can be reached during test, as presented in Figure 8(c). This ignored the response deviation brought by manufacture defect at a certain extent, which partly explains the slightly higher predicted strength.

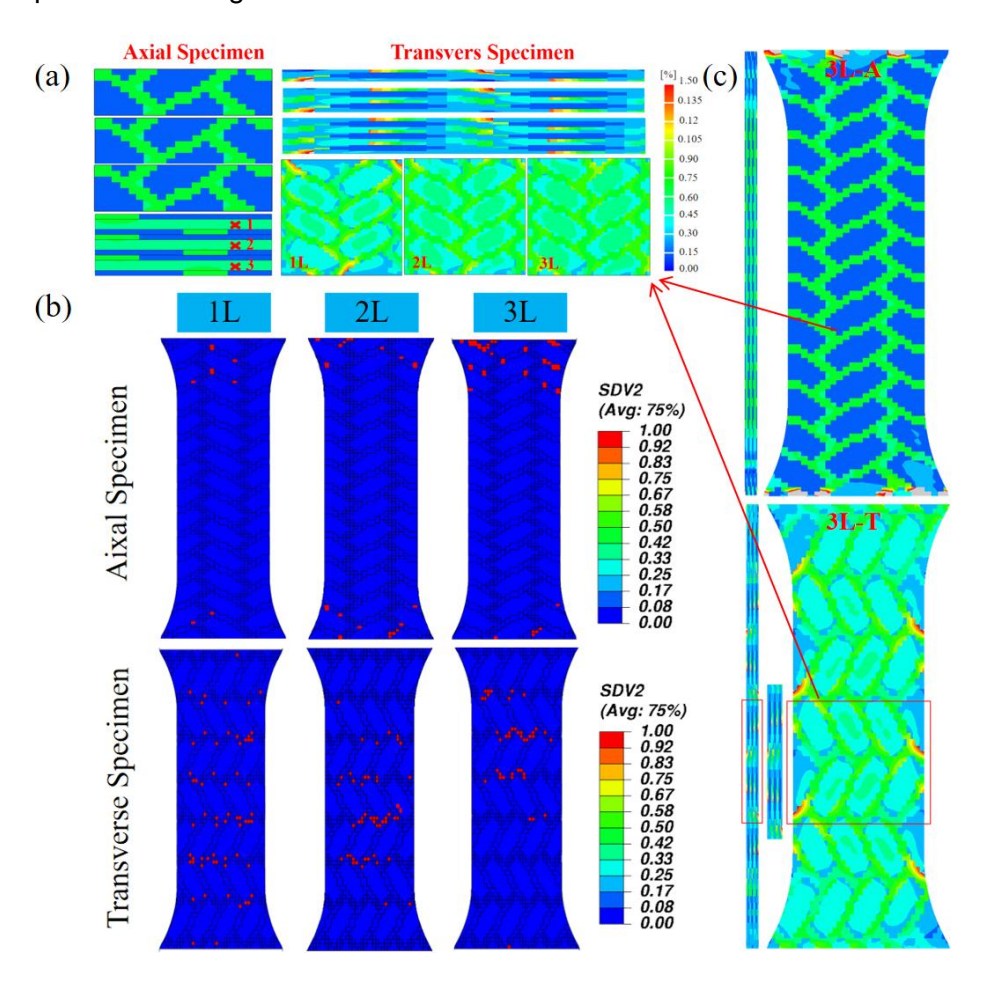


Figure 8-Thickness effect analysis based on the simulating result (a) Localized strain distribution ε_{11} of axial and transverse specimen (b) Failure characterization of fiber tension damage (c) Global strain field of ε_{11} of 2DTBC

5. Conclusions

Quasi-static experiment using the universal test machine was conducted on the 2DTBC specimen with different thickness. The stress-strain curves and failure morphology is compared and characterized. A meso-scale finite element methodology considering the realistic braided architecture and component properties was established to reveal the mechanism of thickness effect on the two dimension triaxial braided composites during tension tests. Impact of thickness effect on the performance discrepancy and failure mechanism is revealed based on the proposed elastoplastic constitutive and FEM results.

Obvious enhancement is found in the strength for both axial specimen and transverse specimen. The strength of axial specimen increases about 20.7%, 28.5% and 35.1% when the layers contained change from 1 layer to 2 layers, 3layers and 8layers, respectively. As for the transverse specimen, the strength increases about 38.5%, 51.1% and 143.4% for 2T, 3T and 8T specimens. Transverse

specimen is more sensitive to the thickness than axial specimen because of the braided architecture and warping behavior caused by reported free-edge effect.

The comparison of final damage morphology indicates that the specimen with higher thickness experiences more damage accumulation and local strain concentration. And the simulating result provides the invisible progressive damage process, where the matrix tension in fiber tow firstly initiates the damage and the crush stage is dominated by the fiber breakage and pure matrix cracking. The more layers the specimen owns, the more and localized damage element appeared which absorbs more energy which explains the better performance of thicker 2DTBC specimen.

Contact Author Email Address

E-mail: Baiyang2000@mail.nwpu.edu.cn

Copyright Statement

The authors confirm that they, and/or their company or organization, hold copyright on all of the original material included in this paper. The authors also confirm that they have obtained permission, from the copyright holder of any third party material included in this paper, to publish it as part of their paper. The authors confirm that they give permission, or have obtained permission from the copyright holder of this paper, for the publication and distribution of this paper as part of the ICAS proceedings or as individual off-prints from the proceedings.

References

- [1] Z. Pan, W. Ouyang, M. Wang, J. Xiao, Z. Wu, In-plane compression failure mechanism of twodimensional triaxial braided composite (2DTBC) material subjected to different load directions, Mech. Mater. 161 (2021) 104001.
- [2] M.R. Wisnom, Size e€ects in the testing of ®bre-composite materials, Compos. Sci. Technol. (1999).
- [3] T. Okabe, Size effect on tensile strength of unidirectional CFRP composites— experiment and simulation, Compos. Sci. Technol. 62 (2002) 2053–2064.
- [4] C. Zhang, W.K. Binienda, R.K. Goldberg, L.W. Kohlman, Meso-scale failure modeling of single layer triaxial braided composite using finite element method, Compos. Part Appl. Sci. Manuf. 58 (2014) 36–46.
- [5] Z. Zhao, P. Liu, C. Chen, C. Zhang, Y. Li, Modeling the transverse tensile and compressive failure behavior of triaxially braided composites, Compos. Sci. Technol. 172 (2019) 96–107. https://doi.org/10.1016/j.compscitech.2019.01.008.
- [6] Y. Cai, Z. Zhao, Y. Tie, Y. Cao, J. Chen, W.K. Binienda, C. Zhang, Size-dependency of the transverse-tensile failure behavior for triaxially braided composites, Compos. Sci. Technol. 206 (2021) 108672.
- [7] P. Liu, Y. Cai, C. Du, Y. Chen, Z. Zhao, C. Zhang, An elastoplastic mechanical-thermal model for temperature rise simulation of two-dimensional triaxially braided composites under quasi-static loads, Compos. Struct. 306 (2023) 116559.
- [8] M. Hu, B. Sun, B. Gu, Microstructure modeling multiple transverse impact damages of 3-D braided

- composite based on thermo-mechanical coupling approach, Compos. Part B Eng. 214 (2021) 108741. https://doi.org/10.1016/j.compositesb.2021.108741.
- [9] T. Belytschko, W.K. Liu, B. Moran, K.I. Elkhodary, Nonlinear finite elements for continua and structures, Second edition, Wiley, Chichester, West Sussex, UK: Hoboken, New Jersey, 2014.
- [10] R. Sun, L. Guo, Z. Li, L. Zhang, T. Zheng, A novel approach to assessing yarn/matrix (or yarn/yarn) in situ interfacial strength in 3D woven composites, Compos. Sci. Technol. 213 (2021) 108893.
- [11] M.L. Benzeggagh, M. Kenane, Measurement of mixed-mode delamination fracture toughness of unidirectional glass/epoxy composites with mixed-mode bending apparatus, Compos. Sci. Technol. 56 (1996) 439–449.
- [12] P. Camanho, Mixed-Mode Decohesion Finite Elements for the Simulation of Delamination in Composite Materials, Compos. Mater. (2002).
- [13] C. Zhang, N. Li, W. Wang, W.K. Binienda, H. Fang, Progressive damage simulation of triaxially braided composite using a 3D meso-scale finite element model, Compos. Struct. 125 (2015) 104–116.
- [14] Y. Bai, H. Wei, J. Gu, Z. Zhao, C. Zhang, Size-dependent mechanical behaviors of 3D woven composite under high strain-rate compression loads, Polym. Test. 127 (2023) 108176.